

Study on Performance Test of Polymer Waterproof Material in Laminated Glass Building Materials of Steel Structure

Tingting Huo^{1,*}, Dawei Fu², Qing Su¹, Feng Zhao¹, Shangjing Zhou¹

¹School of Intelligent Construction, Wuchang University of Technology, Wuhan, China

²China Construction Science and Industry Corporation LTD, Shenzhen, China

*Corresponding author

Abstract: The apparent viscosity, viscosity-flow activation energy and non-Newtonian viscosity of polyvinyl butyral (PVB) were determined by RS150 plate rheometer. The apparent viscosity of PVB water-resistant resin was studied at different shear rates. In this paper, PVB waterproofing agent is used for laminated glass. The bending resistance of PVB waterproof laminated glass is studied. Two different failure forms are summarized: failure forms in steel bars and floating laminated glass. The effect of the PVB waterproof intermediate layer in the test process is compared. The results show that the laminated glass does not have good bending toughness when the thickness of the intermediate film is less than 0.38 mm. The surface viscosity of PVB water-resistant glass decreases with the e-temperature increase. With the increase of shear rate and shear force, the apparent viscosity of PVB waterproof adhesive decreases gradually. Its Newtonian coefficient is less than 1. And it increases as the temperature increases. It indicates that the water-repellent PVB type exists in the form of a pseudo-plastic liquid. The flexural characteristics of various types of PVB waterproof laminated glass are studied. The chemical composition of the PVB water-resistant material sample was analyzed after bending failure. Based on the comparison of component ratio and molecular weight and the conceptual theory of polymer chemistry, the root cause of the failure was explained.

Keywords: Polymer waterproof material, apparent viscosity, laminated glass, polyvinyl butyral, bending property

1. Introduction

Polyvinyl butyral (PVB) has good elasticity and wear and water resistance. It is a new type of waterproof resin with excellent application prospects. There has been a lot of research and development abroad in the 1960s. And it has been popularized in construction and water conservancy^[1]. But because its cost is higher, it somewhat restricts the development of PVB waterproof material. Therefore, much research has been done on PVB waterproof material. Laminated glass is used extensively in contemporary mechanical structures. The flexural capacity is not negligible. At present, laminated glass lining materials are mainly divided into two types: PVB and EVA. In recent years, the ionic transition membrane produced by Coolly Company has been widely used in laminated glass. At present, research on its mechanical properties has become a hot issue. However, our country's research on the flexural property is concise^[2]. Its bending resistance directly affects its mechanical properties and safety. So, we set up a special experimental team and conducted experiments.

The bending properties of glass include two characteristic parameters: the bending strength of glass and the toughness of the intermediate layer material. The bending strength is tested concerning the four-point bracing bending test method in the European standard BSEN1288-3-2000. Stiffness is described in terms of slip in bending tests. Toughness is measured by fracture elongation and fracture condition after a fracture—the broadest range of PVB waterproof laminated glass^[3]. The fractured structure of PVB waterproof laminated glass was studied. In addition, the influence of the thickness of the PVB waterproof plate, sample temperature and PVB waterproof plate on its bending performance is also discussed. This paper has a guiding effect on the waterproof layer, water resistance and durability used in construction engineering.

2. Test materials and equipment

2.1. Materials

Laminated glass production is closely related to production technology. This topic selected several typical architectural glass deep processing companies as the research subject. And use the company's products to produce laminated glass [4]. The product's actual performance is tested according to the manufacturing technology requirements. All the tested samples were tested following the indicators specified in GB/T1563.3 -- 1995. Detailed test film specifications and manufacturers are shown in Table 1 below. In RS150 flat plate rheometer, a certain amount of PVB waterproof substance is added to the sample chamber. The discs are spaced 1.00 mm apart. Rheological properties were measured at 40°C, 50°C, 60°C, 70°C and 80°C.

Table 1: Laminated glass material specifications and list of manufacturers

name	specification
EVA laminated glass	5mmTG+0.76mmEVA+5mmTG
	5mmFG+0.76mmEVA+5mmTG
PVB waterproof laminated glass	5mmTG+0.76mmPVB +5mmTG
	5mmFG+0.76mmPVB +5mmTG
SGP laminated glass	5mmTG+0.76mmSGP+5mmTG
	5mmFG+0.76mmSGP+5mmTG
EVA intermediate membrane	0.76mmEVASAFE®
PVB waterproof intermediate membrane	0.76mm super white all resin
SGP intermediate membrane	0.76mmSentryGlass®

2.2. Test Method

The glass size is 1100mm x 360 mm x 5 mm. 5 laminated glass samples are made at the core of each type. It is necessary to ensure that there is no apparent damage to the surface of the specimen during testing [5]. Assemble and fix the sample as shown in Figure 1. There should be 3mm Shore hardness 40-10 tape between the sample and the bent idler [6]. The working temperature of the flexural performance test must be controlled below 23°C. The relative humidity in the air should be controlled between 40-20%. In the test, only the temperature deviation of the sample is allowed to be 1°C so that the test process is not affected by temperature.

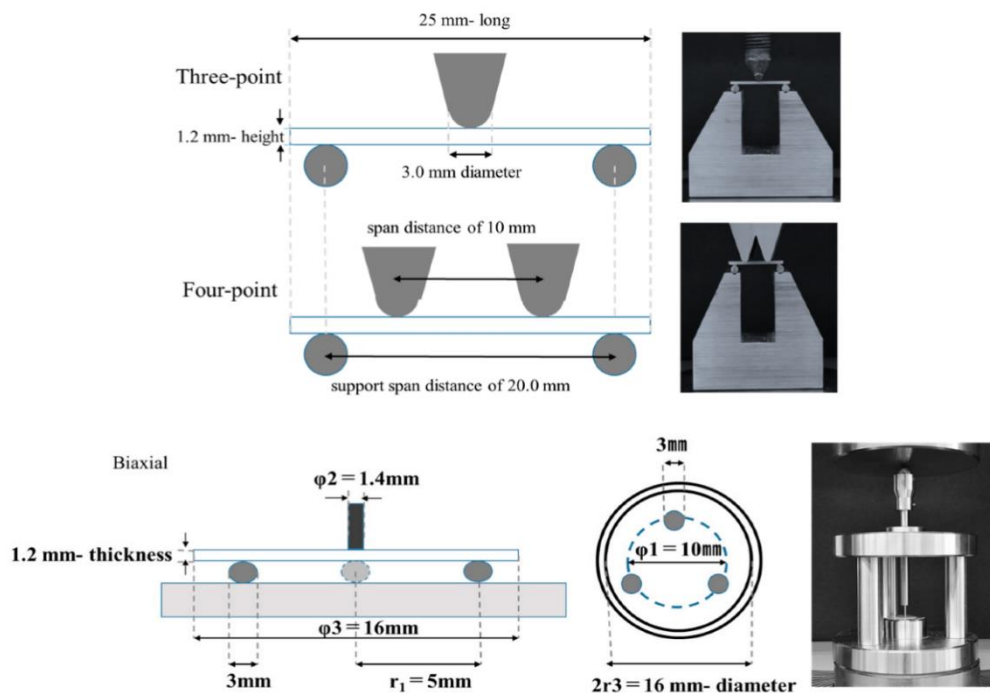


Figure 1: Schematic diagram of installation and fixing of glass bending test sample

The sample should be uniform at (2 ± 0.4) Newtons per square centimeter. The second rate of pressure increases the bending stress of the sample and gradually bends the sample [7]. The maximum F_{max} is recorded along with the load-displacement. After the test, the tangential slip displacements on both sides of the fractured specimens were detected by electron microscopy, and the stiffness of the fractured specimens was evaluated.

2.3. Test the fracture structure of the sample

The broken structure of the sample can be roughly divided into two types. One is a laminated glass with tempered glass as the base material. Another kind of laminated glass is based on available float glass. The hard glass takes on a fish-scale texture when it is broken. The whole glass window was shattered entirely [8]. The float-glass fragments are in strips. The central bend is broken. The rest is in good condition. General schematic Figures 2 and 3 detail the tests.

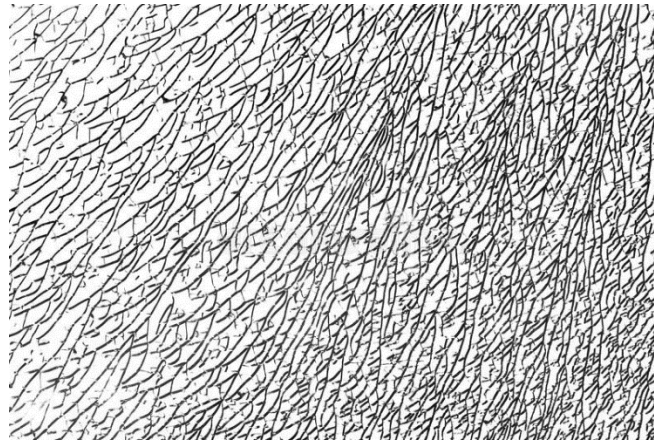


Figure 2: Typical diagram of float laminated glass after failure



Figure 3: Typical diagram of tempered laminated glass after failure

Its failure form is very different from ordinary toughened glass. Float glass cracks are generated from its edges. It's at an Angle to the edge [9]. Typically, the Angle is between 60 and 80 degrees. The results show that a straight crack appears in the toughened glass plate, but there is no apparent relationship between the crack and the Angle of the glass plate.

3. Research on the flexural performance of EVA, PVB and SGP laminated glass

3.1. Test scheme

The maximum load is 0.3 kN for float glass with a thickness of 5 mm. The maximum deformation is 14.0 mm. Bend into a straight line. It depends on the load being added [10]. The bending stress curves of EVA, PVB and SGP are shown in Figure 4. After the bending experiment, the sliding amount of floating laminated glass with three core materials is the same.

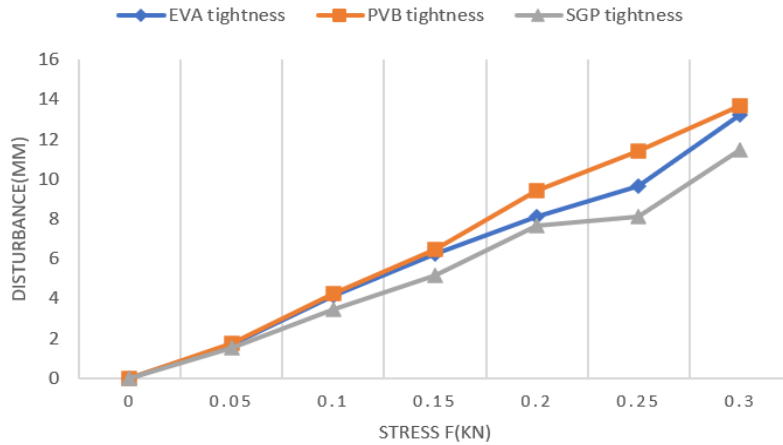


Figure 4: Deflection and stress trends of EVA, PVB and SGP float laminated glass

The bending stress and deflection of EVA, PVB and SGP are similar. Its value is much smaller than the bending strength of ordinary toughened glass. Its mechanical properties primarily determine this. This is because the carrying capacity is too small. The results show that the heat treatment and microstructure stress greatly influence the toughened glass. Float glass is less intense because its annealing process is easier to control. The maximum deformation of float glass is much smaller than that of ordinary tempered glass^[11]. The stress and deflection of EVA, PVB and SGP are different. The most significant factor is the tempered glass itself. The second is the core layer material. The deformation is related to the core material. The test data are presented in Table 2. The deflection and stress variation trends of EVA, PVB waterproof and SGP tempered laminated glass are shown in Figure 5.

Table 2: Statistical tables of bending stress, deflection and sliding displacement of toughened laminated glass of EVA, PVB waterproof and SGP

sample structure	Maximum stress Fmax(kN)	Maximum deflection γ (mm)	sliding displacement μ (mm)
5mmTG+0.76mmEVA+5mmTG	5.83	40.63	0.30
5mmTG+0.76mmPVB+5mmTG	5.73	52.08	0.48
5mmTG+0.76mmSGP+5mmTG	6.88	36.46	0.01
5mmFG+0.76mmEVA+5mmFG	0.33	13.54	0.06
5mmFG+0.76mmPVB +5mmFG	0.32	14.58	0.11
5mmFG+0.76mmSGP+5mmFG	0.34	11.46	0.00

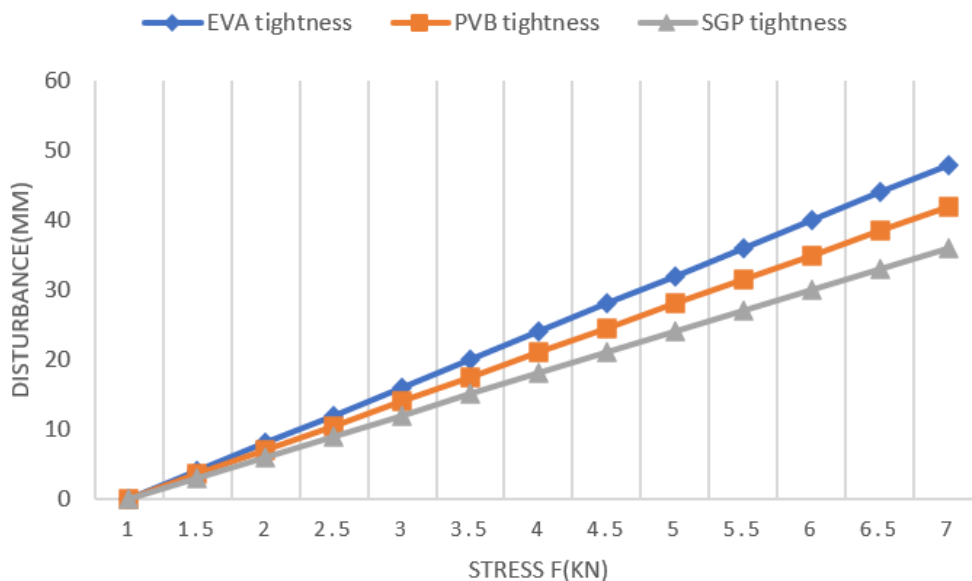


Figure 5: Deflection and stress trends of EVA, PVB and SGP tempered laminated glass

The proportions of EVA, PVB and SGP in the three materials can be roughly estimated from the

analysis of the tabular data. Compared with PVB, the bending deformation difference of EVA is 22.92%. Compared with PVB, the bending deformation difference of SGP is 31.25%. The deviation difference between SGP and EVA is 31.25%. The slip amount of PVB is 1.65 times that of EVA under impervious conditions. Compared with SGP, the anti-slip ability of PVB is increased by 5.67 times. Compared with SGP, the slip amount of EVA is increased by 3.33 times. Compared with EVA, PVB has better water resistance. Its bending strength is only 2.16%. The water resistance of PVB film and SGP film was 17% different. The difference in flexural strength between EVA and SGPP is about 15.63%. From the analysis of the above data, it can be seen that SGP has the minimum relative displacement. The relative displacement of the PVB waterproofing agent is the most significant ^[12]. The same law applies to maximum deformation but not to maximum stress.

The bending strength σ_{bB} is calculated according to the standard formula of BSEN1288-3-2000. Let's calculate σ_{bB} from equation (1). σ_{bB} in formula (1) is the flexural strength caused by the weight of the material. An expression for the calculation of σ_{bG} is given in (2).

$$\sigma_{bB} = k \left[F_{\max} \frac{3(L_s - L_b)}{2Bh^2} + \sigma_{bG} \right] \quad (1)$$

σ_{bB} is the total bending strength, MPa. k is the bending strength coefficient. According to standard BSEN1288-1-2000, $k=1$. F_{\max} is the maximum bending stress, N. According to the standard BSEN1288-3-2000, $L_s=1000\text{mm}$, $L_b=200\text{mm}$. is the width of test sample, mm. h is the total thickness of the test sample, mm. σ_{bG} is its bending strength, MPa.

$$\sigma_{bG} = \frac{3\rho gL_s^2}{4h} \quad (2)$$

ρ is the density of the test material, g/cm^3 . $\rho = 2.4\text{g/cm}^3$, g is the gravitational constant, $g=9.8\text{N/kg}$.

3.2. Impact velocity fitting

In the experiment, the impact head's acceleration, velocity and shift are calculated by integrating the data of the impact force sensor. The calculation method can be seen as follows:

$$V(t) = V_i + \int_0^T A(t)dt = V_i + gT - \int_0^T P(t)dt / m_i \quad (3)$$

$$S(t) = S_i + \int_0^T V(t)dt \quad (4)$$

In the formula, V , A and S are respectively the velocity, acceleration and displacement of the impact head corresponding to a certain time. P is the impact strength. V_i is the incidence rate, and S_i is the initial displacement of the head ^[13]. When the impact head is completely separated from the laminated glass structure, the calculated result is T . m_i is the weight that hits the head. The test results show that this method can obtain P, T value from the impact pressure measured by the gauge. And then we can figure out the bounce rate V_T to determine the bounce rate. Here, it is considered that the process of the impact head falling again and hitting the glass for a second time after impact rebound is in a state of no resistance ^[14]. Then the bounce velocity can be calculated directly from the time T_2 of the second collision. It can be calculated using the following formula:

$$V_T = g(T_2 - T) / 2 \quad (5)$$

In this process, the velocity of an incident wave of ballistic impact wave can be obtained. The flexural strength of EVA, PVB and SGP laminated glass was obtained by the above two formulas combined with the test results. This information is shown in Table 3.

Table 3: Statistical table of bending strength of EVA, PVB waterproof and SGP laminated glass

core layer material	Bending strength (FG)/MPa	bending strength (TG)/MPa
EVA	11.38	169.73
PVB waterproof	11.07	166.72
SGP	11.68	199.71

The bending strength relationships of EVA, PVB waterproof and SGP tempered laminated glass can be sorted out from Table 3, as shown in equation (6). The bending strength of EVA, PVB waterproof glass and SGP float laminated glass is shown in equation (7).

$$\sigma_{bB(EVA)} = 1.018\sigma_{bB(PVB)} = 0.849\sigma_{bB(SGP)} \quad (6)$$

$$\sigma_{bB(EVA)} = 1.027\sigma_{bB(PVB)} = 0.974\sigma_{bB(SGP)} \quad (7)$$

At the end of the experiment, the reinforced, laminated glass was bent differently. In different core materials, its deflection is not the same. This bend is different from the maximum bend. The experimental results show that the deformation value of the laminated glass reinforced by SGP is lower than the maximum deformation value. But the flexural strength of the PVB waterproofing agent and EVA is more significant than its maximum deformation value. The magnitude of the bending quantity is the distance between the reference level and the lowest point of the bending quantity after testing. The flexure of the three conditions is shown in Figure 6.

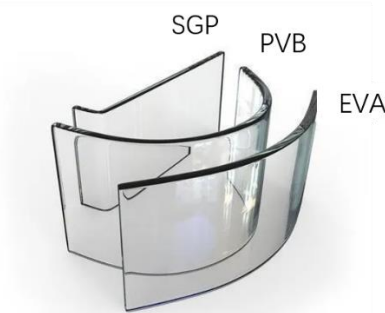


Figure 6: Schematic diagram of bending amplitude of the three tests after standing for 1h

The data analysis in Table 4 shows that the amount of flexure at rest is primarily determined by the mechanical properties of the core material [15]. The corresponding law cannot be obtained from the tensile strength and elongation. According to the hardness of the material, the flexural amplitude is related to the soft property of the material. At room temperature, PVB and EVA are soft rubber plastic films with small hardness and no stiffness. Therefore, the stiffer the SGP, its operational amplitude will be smaller. The flexure value of the hardware and software characteristics is also related to the flexure modulus of the core.

Table 4: List of test data related to bending amplitude of EVA, PVB waterproof and SGP laminated glass

core layer material	Tensile strength /MPa	Fracture elongation /%	Bending amplitude value /mm	Rigid macroscopic performance	Macro performance of toughness	shore D hardness
PVB waterproof	24.58	253.75	89.58	Large bending range	unbroken	34.38
EVA	21.15	469.06	55.21	Moderate bending amplitude	unbroken	27.08
SGP	36.77	316.25	23.96	Small bending amplitude	unbroken	70.83

4. PVB waterproof laminated glass bending performance test research

4.1. Bending test of PVB waterproof laminated glass at different temperatures

The temperature was tested in three stages. The coldest interval is $-30\pm 1^\circ\text{C}$. The average temperature range is $23\pm 1^\circ\text{C}$. The temperature rise is $60\pm 1^\circ\text{C}$. The temperature range for this experiment is based on the temperature range of the extremely cold to scorching world. The specimens and fixed devices to be

tested were placed in high and low-temperature test boxes in advance, and the bending characteristics were tested after constant temperature for 4 hours. The sample size is 1100 mm x 360 mm x 10.76 mm. Its glass characteristics are 5 mm float glass. The results show that the stress of laminated glass can be divided into two kinds under different loading conditions [16]. The short-period load test was carried out. In addition, the flexural characteristics of EVA and SGP were tested respectively under stress and deformation in different temperature ranges. You can see the changes in this data in Figure 7. The test results are shown in Table 5.

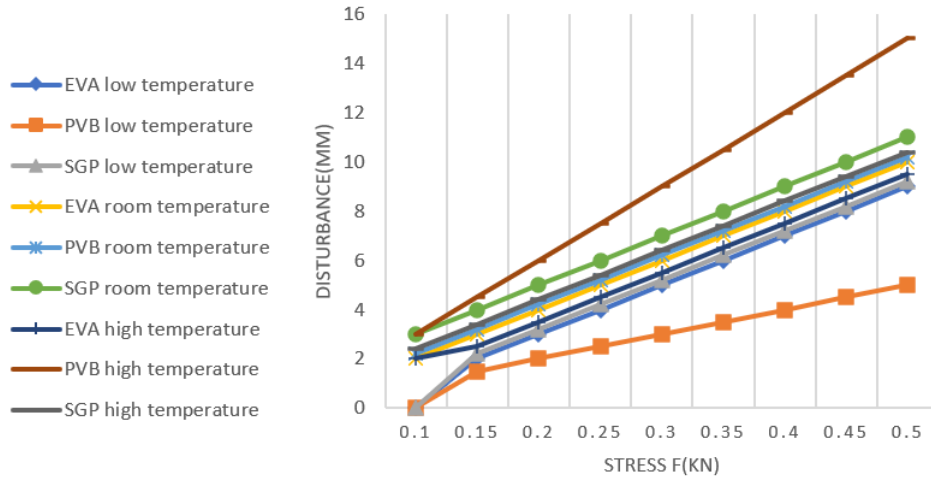


Figure 7: Deflection trend of EVA, PVB waterproof and SGP laminated glass with stress at different temperature segments

Table 5: Statistical table of bending stress, deflection and sliding displacement data of EVA, PVB waterproof and SGP laminated glass at low and high temperatures

test temperature (°C)	Core layer material	Maximum stress Fmax(kN)	Maximum deflection γ (mm)	sliding displacement μ (mm)
-30±1	EVA	0.47	10.00	0.00
	PVB waterproof	0.47	8.33	0.00
	SGP	0.47	10.42	0.00
60±1	EVA	0.32	15.63	0.18
	PVB waterproof	0.31	17.71	0.16
	SGP	0.32	12.50	0.01

In the low-temperature range, the slip amount of the three samples is 0. However, the slip amount of both materials increased at a higher temperature than at room temperature. The PVB water resistance test results of the PVB water resistance test shows all the failure phenomena in the low-temperature range. This phenomenon is caused by the brittleness of the water-resistant intermediate layer of PVB at lower temperatures [17] and is easily broken under the influence of external forces. In the temperature interval test, the cracks produced by the sample during the test differ from those produced by the above test sample. At high temperatures, the water-resistant intermediate layer of PVB is highly elastic. A typical rupture is shown in Figures 8 and 9.



Figure 8: The sample in the low-temperature zone is completely fractured



Figure 9: Fracture lines of samples in a high-temperature area

4.2. Bending performance test of PVB waterproof laminated glass with different thicknesses

At room temperature, EVA, PVB and SGP of the three core materials with a thickness of 0.76mm did not break. This phenomenon is related to the thickness of the core layer. It is only during extrusion that the thickness of the coil is adjusted [18]. The thickness of the PVB impervious intermediate film is set at 0.38 mm, 0.30 mm, 0.20 mm, 0.15 mm and 0.05 mm. The thickness of the last four points is uncertain. The glass used is 5mm float glass. The flexural property of PVB waterproof laminated glass at room temperature was studied. The results are shown in Table 6.

Table 6: Data list after bending test of PVB waterproof laminated glass of different thickness

PVB waterproof thickness /mm	Fracture rate /%	the mean number of fragments after fracture
0.40	10.42	2.08
0.31	31.25	2.08
0.21	52.08	3.13
0.16	83.33	3.65
0.05	104.17	6.25
0.00	104.17	10.42

For data integrity, the bending tests of laminated glass with film thicknesses of 1.14mm, 1.52mm and 2.28mm were added, and the fracture rates were calculated [19]. The fracture trend of PVB waterproof intermediate film thickness from 0 to 2.28mm in the bending test is shown in Figure 10. When the waterproof thickness of PVB is close to 0mm, the performance of laminated glass is close to floating glass. When the PVB waterproof thickness exceeds 0.76mm, the PVB waterproof intermediate film plays the role of buffering and toughening during the bending test. This prevents immediate breakage of the glass.

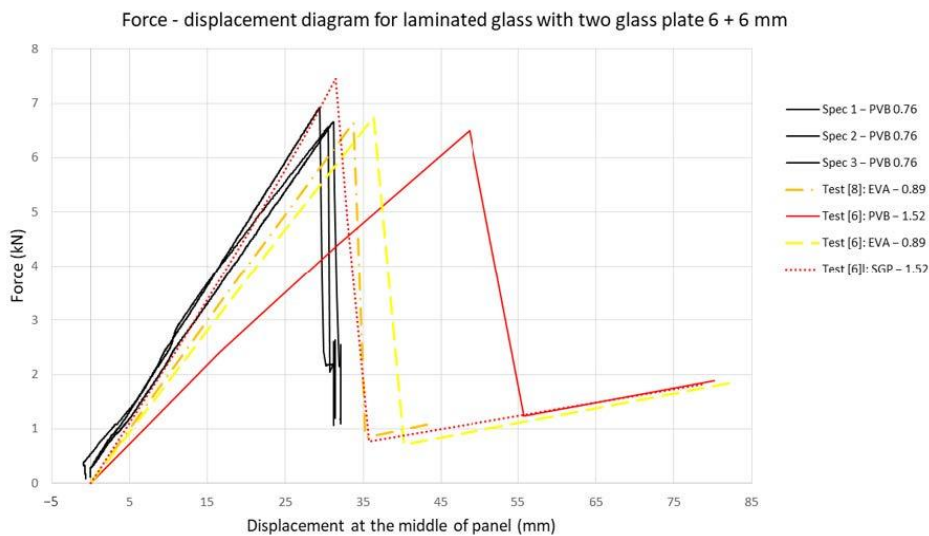


Figure 10: Fracture rate trend diagram of 0mm to 2.28mm PVB waterproof laminated glass in bending test

4.3. Toughness comparison of samples from different manufacturers and failure analysis of fracture samples

Different film manufacturers will appear at different proportions of fracture rates^[20]. For this reason, three PVB waterproofing suppliers were selected for the comparative toughness test. Sample No. 1 is Otenli's entire resin grade. No. 2 is imported film. No. 3 is an ordinary domestic film. Sample No. 3 contains a large amount of recycled material. The tensile strength and fracture elongation of PVB waterproof intermediate film was measured first. The data are shown in Table 7.

Table 7: PVB waterproof bending test and mechanical data of three different manufacturers

sample name	Tensile strength (MPa)	Elongation at break (%)	Bending fracture rate (%)
Sample NO.1	23.64	243.36	10.42
Sample NO. 2	24.91	251.99	8.33
Sample NO. 3	20.49	225.97	52.08

The composition and molecular weight of the three samples were analyzed. The composition analysis is mainly the content analysis of polyvinyl butyraldehyde resin and plasticizer^[21]. The material composition of the three samples is shown in Figure 11. FIG. 12 shows the statistical diagram of components of PVB waterproof interfirm after three kinds of samples were processed by autoclave. The molecular weight test data of gel chromatography are shown in Table 8.

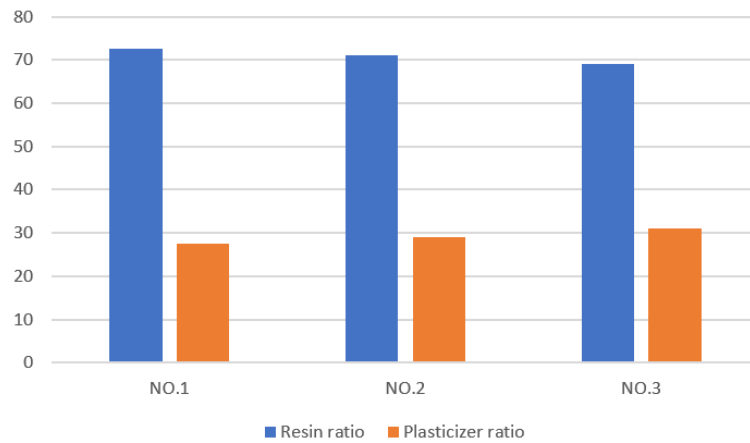


Figure 11: Comparison of PVB waterproofing components from three different manufacturers

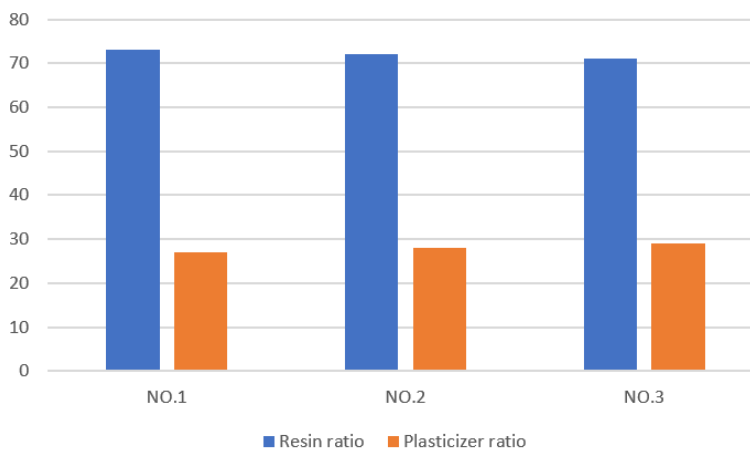


Figure 12: Comparison of PVB waterproofing components in autoclave from three different manufacturers

Table 8: Molecular weight list of PVB waterproof inter film from three different manufacturers

sample name	Mp(g/mol)	Mn(g/mol)	Mw(g/mol)	Mz(g/mol)	(g/mol) Mv	PD
NO.1	106489	59139	179051	440007	396753	3.16
NO.2	118659	64975	204871	490294	442096	3.27
NO.3	88573	34292	84190	157066	147946	2.55

It can be seen from Figures 11, 12 and Table 8 that the plasticizer content of sample No. 3 is slightly higher than that of the other two companies [22]. At the same time, its average molecular weight is lower than the other two. The tensile strength and fracture elongation in mechanical tests are also lower than the others. The plasticizer loss of sample No. 3 was the largest after autoclave processing. According to the above test data and industry experience, the following five reasons for the high failure efficiency of sample No. 3 are analyzed.

- (1) Poor mechanical properties. Tensile strength and elongation at break hover below the national standard line.
- (2) The plasticizer content decreases the overall molecular weight, which cannot provide higher mechanical properties.
- (3) Merchants may add recycled materials. Long-term shear mixing results in weak bond energy and is easy to break.
- (4) Poor heat resistance of the sample. The loss of plasticizer after high temperature and high-pressure lead to the lower toughness of PVB waterproof intermediate film.
- (5) The use of lower molecular weight PVB waterproof resin for blending extrusion.

4.4. Non-Newtonian exponents

From the logarithmic form of the exponential law equation, we know the non-Newtonian exponential $n = \frac{d \ln \tau_w}{d \ln \dot{\gamma}}$. And to figure out n, we have to graph the relationship between $\ln \tau_w$ and $\ln \dot{\gamma}_w$. The relation curve between $\ln \tau_w$ and $\ln \dot{\gamma}_w$ is shown in 13. Non-Newtonian exponents n at different temperatures can be obtained from FIG. 13. The relationship between n and temperature is shown in Table 9.

Table 9: Relationship between n and temperature

t(°C)	40	50	60	70	80
n	0.881	0.945	0.952	0.970	0.994

As can be seen from Table 9, the n value increases as temperature increases. Because the higher the temperature, the more violent the chain motion. Tangles are broken by shear action and re-established by thermal motion [23]. This partially cancels out the shearing. Therefore, the sensitivity of apparent viscosity to shear rate decreases with increasing temperature. The viscous flow activation energy of materials can be expressed in three forms.

The activation energy E_γ at a fixed shear rate is expressed as follows:

$$\eta = A \exp(E_\gamma/RT) \tag{8}$$

The activation energy E_τ under constant shear stress is expressed as follows:

$$\eta = A \exp(E_\tau/RT) \tag{9}$$

The activation energy E_0 in the low-rate Newton region is expressed as follows:

$$\eta_0 = A \exp(E_0/RT) \eta_0 = \lim_{\dot{\gamma} \rightarrow \infty} \eta \tag{10}$$

Usually, E_τ doesn't depend on what happens to τ . And it's close to E_0 . And E_γ decreases as $\dot{\gamma}$ increases. So E_0 is typical. Zero shear viscosity is difficult to measure for most polymer melts and solutions. Therefore, this paper extends its Newton region to $\dot{\gamma} = 10^{-2} s^{-1}$. The viscosity values of samples at different temperatures are obtained and taken as their respective η_0 .

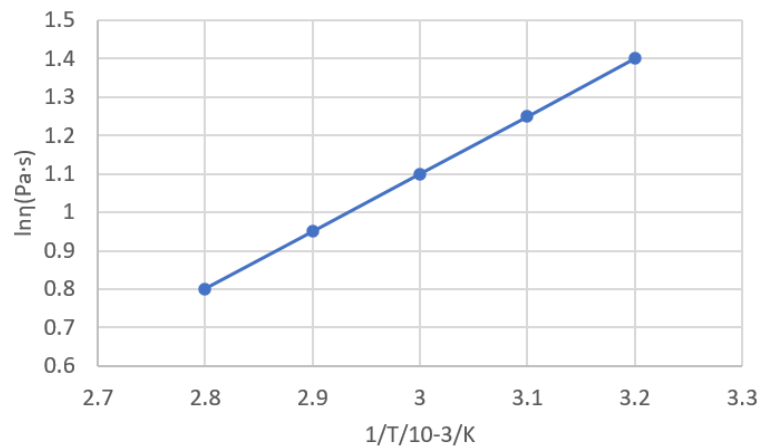


Figure 13: η_0 value is plotted as $\ln \eta_0 - 1/T$

The η_0 value of the sample is made into $(\ln \eta_{0T} - 1)/T$ diagram. It has an excellent linear relationship. The viscous flow activation energy $E_0 = 20.552 \text{ kJ/mol}$ is obtained from the slope.

5. Conclusion

EVA has less bending deformation than SGP. PVB material in impervious conditions slides more. SGP laminated glass has the best bending resistance. PVB waterproof reinforced laminated glass has the most considerable deformation after fracture, while SGP has the most negligible deformation. The mechanical behavior of SGP laminated glass during the test is the best. The water resistance of PVB material is brittle at -30°C . Its float laminated glass does not have the mechanical properties of laminated glass. When the thickness of the water-resistant intermediate layer of PVB is less than 0.38, the breakage rate increases after bending. When its thickness tends to 0, the plasticizing effect will disappear. The conventional thin films containing water-resistant materials of PVB were obtained by comparing the bending and breaking rate of water-resistant materials of various manufacturers. The activation energy of viscous fluid reaches 19.73 kJ/mol when the temperature rises. The improved PVB waterproofing agent has better operability.

Acknowledgements

This work was financially supported by the funds: (1) The Second Batch of Industry-university Cooperative Education Projects in 2021 (202102113047); (2) Hubei Natural Science Foundation Project: Research on the evolution mechanism of bond behavior between rebar and alkali-activated recycled concrete under the influence of corrosion (E2022CFB459); (3) Scientific Research Project: Effect of reclaimed aggregate quality on chloride penetration resistance of reclaimed concrete.

References

- [1] Gong, S., Liang, P., & Cheng, G., (2021). Experimental study on the bearing capacity of glass deck under the condition of vehicle traffic. *Tehnički vjesnik*, 28(3), 796-800.
- [2] Fildhuth, T., & Oppe, M., (2022). Zum Potential unterschiedlicher Methoden beim Einlaminiere n struktureller Metallverbinder. *ce/papers*, 5(3), 1-26.
- [3] Shojaee, T., Mohammadi, B., Pourhosseinsahi, M., & Zeydabadi, I., (2023). Buckling and post-buckling analysis of composite laminates with cutout under compressional loading based on the first-order shear deformation theory. *Acta Mechanica*, 234(5), 2145-2165.
- [4] Imran, M., Shi, D., Tong, L., Waqas, H. M., & Uddin, M., (2021). Design optimization of composite egg-shaped submersible pressure hull for minimum buoyancy factor. *Defence Technology*, 17(6), 1817-1832.
- [5] Eslami, M., Mosalam, K. M., Kodur, V., Marjanishvili, S., Katz, B., & Mahmoud, H. N., (2021). Multi-performance blast pressure-duration curves of laminated glass panes. *International Journal of*

Protective Structures, 12(2), 226-244.

[6] Abdufattoev, D. O., (2022). *The Problem Of Tensioning And Shaping Of Polyvinyl Butyral (Pvb) Film Under The Influence Of Heat Processes In An Autoclave And Directions For Solving*. *Innovative Technologica: Methodical Research Journal*, 3(10), 33-40.

[7] Le Gourriérec, C., Durand, B., Brajer, X., & Roux, S., (2022). *Star Crack Formation via Low-Velocity Impact on Glass Windows*. *Journal of Dynamic Behavior of Materials*, 8(4), 443-452.

[8] Li, D., Zhang, H., Lei, X., Wei, D., & Li, D., (2023). *Three-stage breakage model for laminated glass plate under low-velocity impact*. *Ceramics International*, 49(2), 2648-2662.

[9] Vedrtnam, A., Gunwant, D., Chaturvedi, S., Sagar, D., & Pawar, S. J., (2021). *Experimental and numerical study on abrasive water jet machining of laminated glass*. *Glass Technology-European Journal of Glass Science and Technology Part A*, 62(2), 65-74.

[10] Fildhuth, T., Joos, P., Wüest, T., Haller, M., & Stevels, W., (2022). *Development and behavior of a thin fitting connection for lamination with structural PVB*. *Glass Structures & Engineering*, 7(3), 415-439.

[11] Othman, N. H., Kabay, N., & Guler, E., (2022). *Principles of reverse electrodialysis and development of integrated-based system for power generation and water treatment: A review*. *Reviews in Chemical Engineering*, 38(8), 921-958.

[12] Pan, H., Qu, W., Yang, D., Huang, Q., Li, J., & Ke, Y., (2022). *Design and Optimization of Variable Stiffness Composite Cylinders with the Consideration of Manufacturing Interaction*. *Applied Composite Materials*, 29(3), 1249-1273.

[13] Su, Y., Yang, J., Wang, X., Ma, Y., Pan, D., & Vupputuri, S., (2022). *Surlyn resin ionic interlayer-based laminated glass: preparation and property analysis*. *Advanced Composites and Hybrid Materials*, 5(1), 229-237.

[14] Schuster, M., Thiele, K., & Schneider, J., (2021). *Investigations on the viscoelastic material behaviour and linearity limits of PVB*. *ce/papers*, 4(6), 207-223.

[15] Kaware, K., & Kotambkar, M., (2022). *Low velocity impact response and influence of parameters to improve the damage resistance of composite structures/materials: a critical review*. *International journal of crashworthiness*, 27(4), 1232-1256.

[16] Özdemir Yanık, M. C., Demirel, O., Elmadağlı, M., Günay, E., & Aydın, S., (2023). *Investigation of glass sintering to improve strength and interfacial interactions in glass-to-AISI 316L metal joints*. *International Journal of Applied Glass Science*, 14(2), 256-267.

[17] Gong, S., Liang, P., & Cheng, G., (2021). *Experimental study on the bearing capacity of glass deck under the condition of vehicle traffic*. *Tehnički vjesnik*, 28(3), 796-800.

[18] Hong, S., Kim, Y., & Oh, J., (2022). *Automobile Laminated Glass Window Embedded Transmitarray and Ray Tracing Validation for Enhanced 5G Connectivity*. *IEEE Transactions on Antennas and Propagation*, 70(8), 6671-6682.

[19] Hänig, J., & Weller, B., (2021). *Experimental investigations and numerical simulations of innovative lightweight glass-plastic-composite panels made of thin glass and PMMA*. *Glass Structures & Engineering*, 6(2), 249-271.

[20] Inca 1, E., Jordão 2, S., Bedon 3, C., Mesquita 4, A., & Rebelo 5, C., (2022). *Numerical Analysis of Laminated Glass Panels with Articulated Bolted Point Fixings*. *ce/papers*, 5(2), 140-149.

[21] Fernandes, F. A. O., de Sousa, R. A., & Ptak, M., (2021). *A damage model for the simulation of crack initiation and propagation in automotive windshield laminated glass structures*. *International journal of crashworthiness*, 26(4), 456-464.

[22] Hu, Y., Zhang, Q., Feng, Y., Wan, C., Sun, X., & Duan, J. A., (2023). *The effects of PEG molecular weight on fused silica glass sintering by using nano silicon oxide powder*. *Journal of Sol-Gel Science and Technology*, 105(1), 63-72.

[23] Afluq, S. G., Hachim, M. F., Ibrahim, Z. K., & Alalwan, H. A., (2021). *Reinforcing the mechanical properties of windshield with interlayer-polycarbonates glass composite*. *Journal of Engineering Science and Technology*, 16(5), 4192-4204.